Optical properties of diamond

A. D. Papadopoulos and E. Anastassakis
Physics Department, National Technical University, GR-157 73 Zografou, Greece
(Received 5 June 1990)

The optical properties of diamond are examined in the energy region up to 25 eV. A modified parabolic-band model is used to explain existing experimental data on the dispersion of the real and imaginary part of the dielectric function. Optical properties such as reflectance, index of refraction, and extinction coefficient are also determined in the same region.

I. INTRODUCTION

Diamond is one of the basic classical materials in the sense that its simple covalent band structure serves as a model for the study of fundamental electronic properties of crystals. The interest in diamond has revived in recent years because of advances in the production of diamond thin films by chemical vapor deposition or other methods, an important development in optical and electronic technologies.[1] Ample information about the electronic band structure of diamond has been obtained through the study of its optical properties.[2,3] The present contribution concerns such properties in the energy region up to 25 eV.

The optical properties of solids are most fundamentally described by their complex dielectric function $\epsilon(\omega)=\epsilon_r(\omega)+i\epsilon_i(\omega)$. The two parts of $\epsilon(\omega)$ can be derived from the reflectance spectrum by use of the Kramers-Kronig relations.[4] The reflectance and absorption spectra of all diamond- and zinc-blende-type semiconductors are known to exhibit similar structures, which are well understood and attributed to interband electronic transitions.[5–7] Korovin first explained the dispersion of optical constants of semiconductors near the direct absorption edge using a classical oscillator model.[8] Cardona developed a model based on the joint density of states and included contributions from the indirect as well as the main direct gaps.[9,10] Higginbotham *et al.*,[11] and more recently Adachi,[12] improved the previous model by introducing the so-called parabolic-band model (PBM) which explains adequately the optical spectra of group IV, III-V, and II-VI semiconductors.[12–14] Other models have also been proposed by Marple and Ehrenreich,[15] Stern,[16] Wemple and DiDomenico,[17] and Pikhtin and Yas'kov.[18]

We have used a modified PBM model to account for existing data on the dispersion of optical constants of diamond in the energy region up to 25 eV. Our approach consists in taking into account broadening effects to the real and imaginary part of the dielectric function for all major contributing energy gaps. In addition, we have included similar contributions arising from the electronic plasma. The latter contributions turn out to be of importance in the high-energy region, i.e., beyond 15 eV. In planning, Sec. II describes the extended PBM used here, while its application to diamond and all related results are presented in Sec. III. To our knowledge, no similar study has been previously reported for diamond, covering the energy region considered here.

II. THEORETICAL CONSIDERATIONS

The reflectance spectra of all semiconductors with diamond and zinc-blende structure exhibit similarities due to characteristic peaks, which correspond to certain energy gaps denoted by $E_{\rm ID}$ (indirect), E_0, E_0', E_1, E_1', E_2, etc. From the behavior of $\epsilon_r(\omega)$ and $\epsilon_i(\omega)$ in the vicinity of these peaks it is possible to learn how such peaks are associated with specific interband critical points (CP's).[10,19] Next we examine the independent contributions of these gaps to the dielectric function, starting with the PBM formulation which we then extend according to the present approach.

A. E_0 and E_0' gaps

The E_0 ($\Gamma_{25'}^v\rightarrow\Gamma_{2'}^c$) and E_0' ($\Gamma_{25'}^v\rightarrow\Gamma_{15}^c$) direct gaps and the corresponding spin-orbit split gaps $E_0+\Delta_0$ and $E_0'+\Delta_0'$ appear in the $\epsilon_i(\omega)$ spectrum as absorption edges and in the $\epsilon_r(\omega)$ spectrum as sharp peaks. In most cases they are recognized as three-dimensional minima CP (M_0 type). According to the PBM, the contribution of each gap to $\epsilon_i(\omega)$ is of the form[20]

$$[\epsilon_i(\omega)]_0=A_0\left[f_i(x_0)+\frac{1}{2}\left[\frac{\omega_0}{\omega_{0s}}\right]^{3/2}f_i(x_{0s})\right], \quad (1)$$

where ω_0 corresponds to the energy of either of the gaps (E_0 or E_0') and ω_{0s} corresponds to the energy of their spin-orbit split counterparts ($E_0+\Delta_0$ or $E_0'+\Delta_0'$); by definition $x_0=\omega/\omega_0$ and $x_{0s}=\omega/\omega_{0s}$. The coefficient A_0 stands for $\frac{4}{3}P^2(2\mu^*/\omega_0)^{3/2}$, where μ^* is the average reduced mass of the electron-hole pairs and P^2 is an average momentum matrix element. The function f_i is defined by

$$f_i(x)=\frac{(x-1)^{1/2}}{x^2}H(x-1), \quad (2)$$

where H is the step function

$$H(y)=\begin{cases}0 & \text{for } y<0\\ 1 & \text{for } y\geq 0.\end{cases} \tag{3}$$

Likewise, the contribution of these gaps to $\epsilon_r(\omega)$ has the form

$$[\epsilon_r(\omega)-1]_0=A_0\left[f_r(x_0)+\frac{1}{2}\left[\frac{\omega_0}{\omega_{0s}}\right]^{3/2}f_r(x_{0s})\right], \tag{4}$$

where

$$f_r(x)=x^{-2}[2-(1+x)^{1/2}-(1-x)^{1/2}H(1-x)]\ . \tag{5}$$

Contrary to $f_r(x)$ itself, its first derivative is discontinuous at $x=1$. The discontinuity is removed if broadening effects of phonons, lattice defects, and impurities are introduced in Eq. (4). Phenomenologically, this is most effectively done by replacing $\omega+i\Gamma$ for ω and taking the real part of the resultant expression.[9] Γ is an appropriate width in energy units. Application to the E_1 gap alone has been presented by Adachi in a number of III-V and group IV materials.[12–14] We have applied this approach to Eq. (4) by replacing $\omega+i\Gamma_0$ ($\omega+i\Gamma_{0s}$) for ω in the first (second) term inside the square brackets of Eq. (4). The resulting expression is

$$[\epsilon_r(\omega)-1]_0=A_0\left[f_{rb}(x_0,\gamma_0)+\frac{1}{2}\left[\frac{\omega_0}{\omega_{0s}}\right]^{3/2}f_{rb}(x_{0s},\gamma_{0s})\right], \tag{6}$$

where $\gamma_0=\Gamma_0/\omega_0$, $\gamma_{0s}=\Gamma_{0s}/\omega_{0s}$, and

$$f_{rb}(x,\gamma)=(x^2+\gamma^2)^{-2}\{(x^2-\gamma^2)[2-F(1+x,\gamma)-F(1-x,\gamma)]-2\gamma x[F(-x-1,\gamma)-F(x-1,\gamma)]\}\ , \tag{7}$$

with

$$F(y,\gamma)=\left[\frac{y+(y^2+\gamma^2)^{1/2}}{2}\right]^{1/2}. \tag{8}$$

The function $f_{rb}(x,\gamma)$ is shown in Fig. 1 for various values of γ. By definition, $f_{rb}(x,0)$ is equal to $f_r(x)$ of Eq. (5).

Next we examine how the broadening energy affects the contributions of E_0 and E_0' to $\epsilon_i(\omega)$. Upon substituting $\omega+i\Gamma_0$ ($\omega+i\Gamma_{0s}$) for ω in the first (second) term inside the square brackets of Eq. (1), we find for the real part,

$$[\epsilon_i(\omega)]_0=A_0\left[f_{ib}(x_0,\gamma_0)+\frac{1}{2}\left[\frac{\omega_0}{\omega_{0s}}\right]^{3/2}f_{ib}(x_{0s},\gamma_{0s})\right], \tag{9}$$

where

$$f_{ib}(x,\gamma)=(x^2+\gamma^2)^{-2}[(x^2-\gamma^2)F(x-1,\gamma)+2\gamma xF(-x+1,\gamma)]\ . \tag{10}$$

With γ being small compared to unity, Eq. (10) diverges as $x\rightarrow 0$ because of the term $(x^2+\gamma^2)^{-2}$; this is contrary to the observed dispersion of $\epsilon_i(\omega)$ below the absorption edge. However, we are interested in the dispersion of $\epsilon_i(\omega)$ in the region just below ($x\lesssim 1$) and above ($x\geq 1$) the absorption edge. For this reason we construct the function

$$f_{ib}'(x,\gamma)=\frac{(x^2-\gamma^2)F(x-1,\gamma)-2\gamma xF(-x+1,\gamma)}{[1+(x^2+\gamma^2-1)H(x^2+\gamma^2-1)]^2}\ , \tag{11}$$

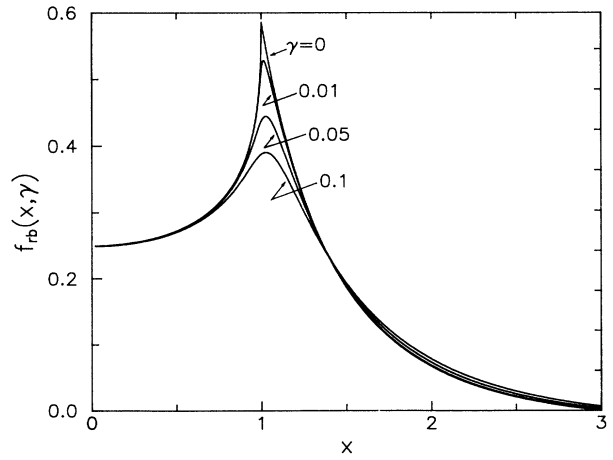

FIG. 1. The function $f_{rb}(x,\gamma)$ of Eq. (7) for various values of the parameter γ.

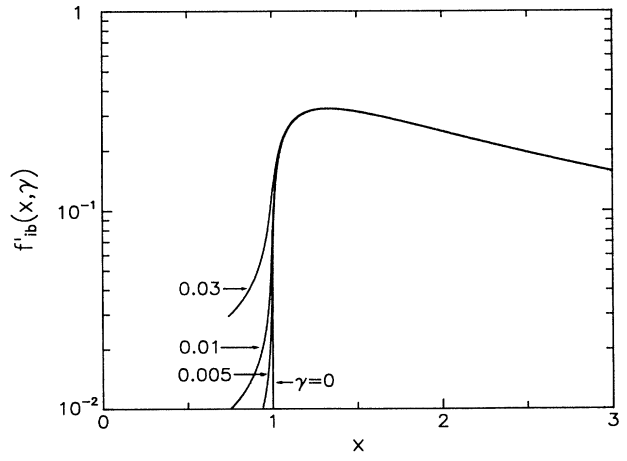

FIG. 2. The function $f_{ib}'(x,\gamma)$ of Eq. (11) for various values of the parameter γ.

which coincides with $f_{ib}(x,\gamma)$ for $x \geq 1$ and is very close to it for $x \lesssim 1$. Under these conditions Eq. (11) represents fairly well the dispersion of $\epsilon_i(\omega)$ in the region of interest. In Fig. 2, $f'_{ib}(x,\gamma)$ has been plotted for various values of γ. By definition, $f'_{ib}(x,0)$ is equal to $f_i(x)$ of Eq. (2). Finally, Eq. (9) becomes

$$[\epsilon_i(\omega)]_0 = A_0 \left[f'_{ib}(x_0,\gamma_0) + \frac{1}{2} \left[\frac{\omega_0}{\omega_{0s}} \right]^{3/2} f'_{ib}(x_{0s},\gamma_{0s}) \right] . \tag{12}$$

B. E_1 and E'_1 gaps

The E_1 ($L^v_{3'} \rightarrow L^c_1$, $\Lambda^v_3 \rightarrow \Lambda^c_1$) and E'_1 ($L^v_{3'} \rightarrow L^c_3$, $\Lambda^v_3 \rightarrow \Lambda^c_3$) direct gaps and their spin-orbit split counterparts $E_1+\Delta_1$ and $E'_1+\Delta'_1$ manifest themselves in the $\epsilon_r(\omega)$ and $\epsilon_i(\omega)$ spectra as peaks, usually above the lowest direct gap (E_0 or E'_0). In most of the cases they are recognized as three-dimensional M_1-type CP. However, the longitudinal effective mass along the [111] direction is much larger than the transverse effective masses; one can then approximate these three-dimensional CP by two-dimensional minima (P_0 type).[11] The contributions of these gaps to the imaginary and real part of the dielectric function, without any broadening included, are given by[20]

$$[\epsilon_i(\omega)]_1 = \pi A_1 x_1^{-2} H(x_1-1) + \pi A_{1s} x_{1s}^{-2} H(x_{1s}-1) , \tag{13}$$

$$[\epsilon_r(\omega)-1]_1 = A_1 L(x_1) + A_{1s} L(x_{1s}) , \tag{14}$$

where $x_1=\omega/\omega_1$ and $x_{1s}=\omega/\omega_{1s}$; ω_1 corresponds to the energy of either of the two gaps (E_1 or E'_1) and ω_{1s} corresponds to the energy of their spin-orbit split counterparts ($E_1+\Delta_1$ or $E'_1+\Delta'_1$). The function $L(x)$ is defined by

$$L(x) = -x^{-2}\ln|1-x^2| . \tag{15}$$

This latter function diverges at $x=1$ contrary to the experimental data for $\epsilon_r(\omega)$. If, however, broadening effects are taken into account the function becomes finite at $x=1$. We incorporate these effects into Eq. (14) in the same phenomenological manner as before, i.e., by replacing $\omega+i\Gamma_1$ ($\omega+i\Gamma_{1s}$) for ω in the first (second) term of the right-hand side of Eq. (14). The resulting expression is

$$[\epsilon_r(\omega)-1]_1 = A_1 L_b(x_1,\gamma_1) + A_{1s} L_b(x_{1s},\gamma_{1s}) , \tag{16}$$

where $\gamma_1=\Gamma_1/\omega_1$, $\gamma_{1s}=\Gamma_{1s}/\omega_{1s}$ and

$$L_b(x,\gamma) = -(x^2+\gamma^2)^{-2} \left[\frac{1}{2}(x^2-\gamma^2)\ln[(x^2-\gamma^2-1)^2+4x^2\gamma^2] + 2\gamma x \arctan\left[\frac{2\gamma x}{x^2-\gamma^2-1} \right] \right] . \tag{17}$$

The arctan is defined in the region $(-\pi,0]$. In Fig. 3, we show plots of $L_b(x,\gamma)$ for various values of γ. By definition, $L_b(x,0)$ is equal to $L(x)$ of Eq. (15). Inclusion of broadening in Eq. (13) does not change significantly the form of this function.

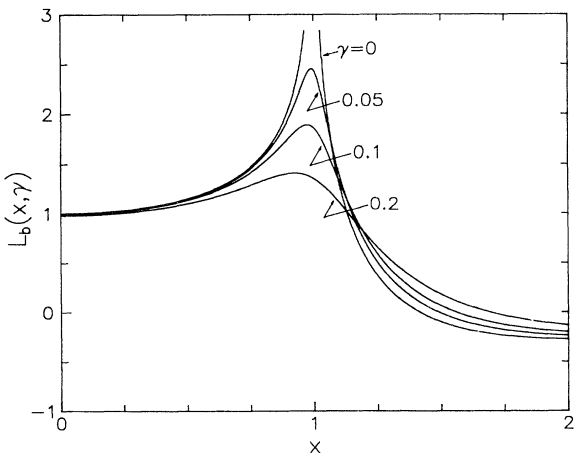

FIG. 3. The function $L_b(x,\gamma)$ of Eq. (17) for various values of the parameter γ.

C. E_2 gap

The E_2 gap is represented by an intense broadband in the spectra of $\epsilon_i(\omega)$ for all diamond- and zinc-blende-type semiconductors. It is attributed mainly to transitions at the X point of the Brillouin zone.[6,7] From the behavior of $\epsilon_r(\omega)$ and $\epsilon_i(\omega)$ around this point, the E_2 gap is recognized as a two-dimensional saddle CP (P_1 type). Furthermore, Adachi has shown[13] that it can be represented by an effective damped harmonic oscillator with contributions to $\epsilon_r(\omega)$ and $\epsilon_i(\omega)$, which are given by the standard functions[21]

$$[\epsilon_r(\omega)-1]_2 = A_2 \frac{(1-x_2^2)}{(1-x_2^2)^2+\gamma_2^2 x_2^2} , \tag{18}$$

and

$$[\epsilon_i(\omega)]_2 = A_2 \frac{\gamma_2 x_2}{(1-x_2^2)^2+\gamma_2^2 x_2^2} . \tag{19}$$

Here $x_2=\omega/\omega_2$, where ω_2 corresponds to the energy of the E_2 gap. A_2 is the strength of the oscillator and γ_2 is a damping parameter.

D. E_{ID} gap

The E_{ID} gap corresponds to indirect transitions. Because such transitions involve weak second-order pro-

cesses, their observation is possible only in frequency regions which are free of other strong processes.[10] This means that $E_{\rm ID}$ can be observed in the $\epsilon_i(\omega)$ spectrum as an absorption edge only if it happens to be the lowest gap of the material (e.g., C, Si, Ge, and GaP). The contribution of $E_{\rm ID}$ to $\epsilon_r(\omega)$ is considered negligible,[10] while its contribution to $\epsilon_i(\omega)$ has the form[22,10]

$$[\epsilon_i(\omega)]_{\rm ID}=A_{\rm ID}\left[1-\frac{1}{\bar{x}_{\rm ID}}\right]^2 H(\bar{x}_{\rm ID}-1)\ , \tag{20}$$

where $\bar{x}_{\rm ID}=\omega/(\omega_{\rm ID}\pm\omega_{\rm phon})$. Here $\omega_{\rm ID}$ corresponds to the energy of the indirect gap (energy difference between the initial and final states of the transition) and $\omega_{\rm phon}$ is the energy of the phonon involved in the transition. The $+$ $(-)$ sign corresponds to phonon emission (absorption). The coefficient $A_{\rm ID}$ is proportional to the Bose-Einstein function $f_B(\omega_{\rm phon}/T)$ for phonon absorption, and to f_B+1 for phonon emission.

The indirect transitions are usually modified by exciton effects, at least for the indirect gap materials mentioned above. In this case, the contribution of the $E_{\rm ID}$ gap to $\epsilon_{\rm ID}(\omega)$ is similar to that of an M_0-type CP,[10] which has already been encountered and discussed in Eq. (1), but without the spin-orbit term, i.e.,

$$[\epsilon_i(\omega)]_{\rm ID}=A_{\rm ID}f_i(\bar{x}_{\rm ID})\ , \tag{21}$$

where $\bar{x}_{\rm ID}=\omega/(\omega_{\rm ID}-E_{\rm ex}\pm\omega_{\rm phon})$. Here $E_{\rm ex}$ is the binding energy of the indirect exciton. We see that the exciton and phonon energies result in shifting of the absorption edge below the indirect gap energy. The amount of shift and the overall band shape is modified when we include broadening effects in Eq. (21), as was done in Eq. (1). We then find for the contribution of $E_{\rm ID}$ to $\epsilon_i(\omega)$,

$$[\epsilon_i(\omega)]_{\rm ID}=A_{\rm ID}f'_{ib}(\bar{x}_{\rm ID},\bar{\gamma}_{\rm ID})\ , \tag{22}$$

where $\bar{\gamma}_{\rm ID}=\Gamma_{\rm ID}/(\omega_{\rm ID}-E_{\rm ex}\pm\omega_{\rm phon})$. In this case, no plotting is necessary for Eq. (22) in view of Fig. 2.

III. OPTICAL PROPERTIES OF DIAMOND

A. Available data

Diamond is an indirect gap material with $E_{\rm ID}$ at 5.47 eV; the absorption at this energy rises abruptly by several orders of magnitude.[2,23] Natural diamonds can be classified in various classes according to their infrared and far-ultraviolet optical properties. Type-I diamonds (most natural diamonds are of this type) absorb light at three distinct bands around 0.15, 0.25, and 0.41 eV (Ref. 24) with a secondary absorption edge around 4 eV.[25] This behavior is mainly due to nitrogen impurities.[26] In type-IIa and -IIb diamonds the 0.15-eV band and the second absorption edge are absent; type-IIb diamonds (semiconducting diamonds) phosphoresce in the far ultraviolet, exhibit electrical conductivity[27] and a rich impurity-induced absorption spectrum in the infrared.[28] Furthermore, types I and II show different behavior in photoconductivity.[24] Type-IIa diamonds are considered most pure and representative of the ideal diamond crystal.

Here we are interested in the optical properties of diamond in the ultraviolet, i.e., for energies greater than the fundamental absorption edge. In this region, types I and IIa show similar behavior[3] and their properties have been studied experimentally by many workers; as a result ample information is available. The reflectance spectra of type-I and -IIa crystal samples, in particular, have been repeatedly reported. The real and imaginary parts of the dielectric function can be inferred from such spectra.

One common characteristic of all published reflectance spectra is the presence of two major peaks. Nelson and Crocker[29] observed these peaks at 7.19 and 12.7 eV, Philipp and Taft[30,2] at 7.1 and 12.5 eV, Clark *et al.*[23] at 7.02 and 12.5 eV, Walker and Osantowski[31] at 7.4 and 12.6 eV, and Roberts and Walker[3] at 7.2 and 12.2 eV. The evaluation of the dispersion of the real and imaginary parts of the dielectric function through Kramers-Kronig analysis[2,3] has made it clear that the first peak originates from $\Gamma^v_{25'}\rightarrow\Gamma^c_{15}$ transitions (direct gap E'_0), and the second one from $X^v_4\rightarrow X^c_1$ and $\Sigma^v_2\rightarrow\Sigma^c_3$ transitions (E_2 gap). This assignment is also supported by Armon and Sellschop,[32] who measured the angular dependence of electron-energy-loss spectra of a type-IIa sample and observed structures at 6.5 ± 1.0 and 12.5 ± 0.5 eV.

The positions of the E_1 and E'_1 gaps are rather uncertain. Clark *et al.*[23] and Roessler[33] have observed a broad peak in the reflection spectrum of diamond around 9.2 eV which, however, has not been confirmed by other researchers. On the other hand, band-structure calculations by Saslow *et al.*[34] and by Herman *et al.*[35] place the E_1 and E'_1 gaps near 11 eV, where the E_2 structure dominates. This might explain the absence of any E_1 and E'_1 peaks from the reflectance spectrum. Structure has also been observed around 16 eV (Refs. 2, 31, 32, and 36) (assigned to the $X^v_1\rightarrow X^c_1$ transition[3] or to the $\Gamma^v_{25'}\rightarrow\Gamma^c_{2'}$ transition,[36] namely, to the E_0 gap) and around 24 eV (Refs. 2, 3, 31, 32, and 36) (assigned to the $\Gamma^v_{25'}\rightarrow\Gamma^c_1$ transition[27]). Finally, the free electron plasma resonance for diamond has been placed at $\omega_p=31$ eV, according to the electron-energy-loss curve $-\mathrm{Im}(1/\epsilon)$ calculated from the optical constants[3] and, independently, from electron-energy-loss measurements.[37]

From all the available experimental results we have chosen to use those of Philipp and Taft[2] which practically coincide with the data of Roberts and Walker[3] and provide values for the absorption coefficient in the region immediately above the fundamental absorption edge. The secondary peak of reflectance observed by Roberts and Walker[3] around 7.6 eV is absent in Ref. 2. It should be noted, however, that in their earlier reflectivity data, Philipp and Taft[30] mentioned the possibility of a small peak present near 7.7 eV. Its magnitude was within the estimated uncertainty limits of the data and was not taken into account (it occurred in a region of rapid change in the hydrogen-arc spectral intensity). Furthermore, the theoretical calculations on the band structure of diamond[34,35] do not predict any transition around 7.6 eV. Finally, it should be mentioned that the reflectance spectrum by Philipp and Taft[2] was obtained with a type-I sample. As Walker and Osantowski[31] and Roberts and Walker[3] have shown independently, type-IIa diamonds

yield reflectance spectra very similar in structure but lower in strength than those of type I (about 50% and 60%, respectively). In none of these studies has any fitting to the data been undertaken over the entire region from 0 to 25 eV.

B. Fitting procedure

In the remainder of this work, the experimental data on the dispersion of the optical constants of diamond will be described by use of the extended PBM presented in Sec. II. The experimental curves for the real and imaginary parts of the dielectric function given by Philipp and Taft[2] were first digitized in the energy region up to 25 eV and represented by 94 points. These points are shown in Figs. 4 and 5, respectively, on a linear scale. The values of $\epsilon_r(\omega)=n^2(\omega)$ below 5.5 eV were calculated from Sellmeier's formula[38,2]

$$n^2-1=\frac{a\lambda^2}{\lambda^2-\lambda_1^2}+\frac{b\lambda^2}{\lambda^2-\lambda_2^2}\ , \tag{23}$$

where $a=0.3306$, $b=4.3356$, $\lambda_1=175$ nm, and $\lambda_2=106$ nm. The values of $\epsilon_i(\lambda)$ just above the fundamental absorption edge were calculated from the absorption coefficient $\alpha(\lambda)$ of Philipp and Taft,[2] using the relation[21]

$$\epsilon_i(\lambda)=\frac{\alpha(\lambda)\lambda}{2\pi}\left[\epsilon_r(\lambda)+\left[\frac{\alpha(\lambda)\lambda}{4\pi}\right]^2\right]^{1/2}\ . \tag{24}$$

The entire set of $\epsilon_i(\omega)$ points is shown in Fig. 6 on a logarithmic scale. The two absorption edges are clearly seen. The first, around 5.5 eV, is due to the indirect gap ($E_{\rm ID}$), and the second, around 7.1 eV, to the direct gap (E_0'). Clark *et al.*[23] place the indirect gap at 5.47 eV. They have also found that the indirect exciton binding energy is 0.07 eV and the energy of the phonons involved in the transition are of the order of 0.1 eV. Thus the observation of Philipp and Taft[2] that the absorption commences at about 5.3 eV is in accordance with the above findings, implying that $\omega_{\rm ID}=5.47$ eV is a reasonable choice. Likewise, we infer the position of the direct gap from the maximum of the sharp peak of $\epsilon_r(\omega)$ at 7.1 eV (Philipp and Taft[2] themselves place it near 7.3 eV). The spin-orbit splitting of this gap is 0.006 eV,[39] i.e., much smaller than E_0'. Therefore $\omega_{0s}\simeq\omega_0$, and Eqs. (1), (12), (4), and (6) are simplified as follows:

$$[\epsilon_i(\omega)]_0'=\tfrac{3}{2}A_0 f_i(x_0)\ , \tag{25}$$

$$[\epsilon_i(\omega)]_0'=\tfrac{3}{2}A_0 f_{ib}'(x_0,\gamma_0)\ , \tag{26}$$

$$[\epsilon_r(\omega)-1]_0'=\tfrac{3}{2}A_0 f_r(x_0)\ , \tag{27}$$

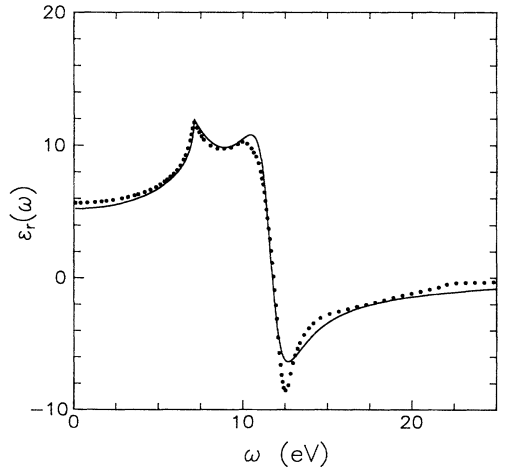

FIG. 4. Energy dispersion of the real part of the dielectric function of diamond. Dots: experimental points (after Ref. 2). Solid curve: results of fitting of the sum of Eqs. (18), (28), and (29) to the data.

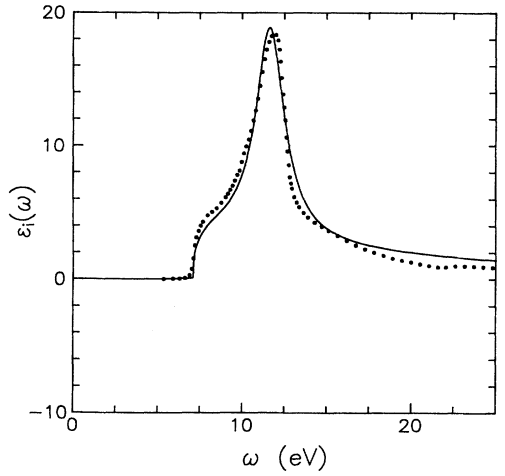

FIG. 5. As in Fig. 4 for the imaginary part of the dielectric function of diamond, above the fundamental absorption edge. Solid curve: results of fitting of the sum of Eqs. (22), (30), and (31) to the data.

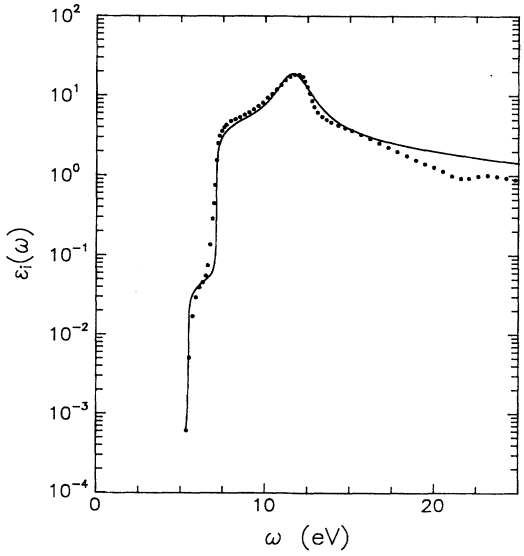

FIG. 6. As in Fig. 5 for the imaginary part of the dielectric function of diamond, on a logarithmic scale.

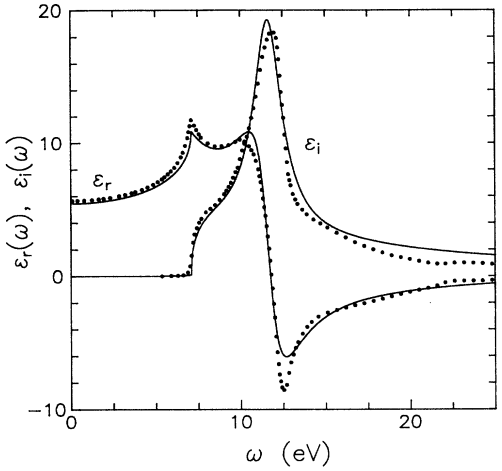

FIG. 7. As in Figs. 4 and 5 for the real and imaginary part of the dielectric function of diamond after simultaneous fitting.

$$[\epsilon_r(\omega)-1]_0'=\tfrac{3}{2}A_0 f_{rb}(x_0,\gamma_0)\ , \tag{28}$$

respectively. It is also noted that in our model we have ignored any contributions from the experimental structures at 16 and 24 eV, as we are only concerned with effects arising from the primary gaps.

The data points for $\epsilon_r(\omega)$ were first fitted by the sum of Eqs. (28) and (18), with $\omega_0=7.1$ eV and A_0, γ_0, ω_2, A_2, and γ_2 as free parameters. A background constant A_c was added to account for the contribution of all other gaps. The value found for A_c was negative (-1.7). We attribute this to a contribution of the plasma electrons; the latter is expressed by the well-known Drude formula

$$[\epsilon_r(\omega)-1]_p=-\frac{1}{x_p^2+\gamma_p^2}\ , \tag{29}$$

where $x_p=\omega/\omega_p$ and γ_p is an appropriate damping constant. We have therefore repeated the fitting with Eq. (29) substituting for the background constand A_c. The values of the parameters found are presented in the second column of Table I. The results are shown by solid lines in Fig. 4.

Because of the abrupt rise of $\epsilon_i(\omega)$ above both $E_{\rm ID}$ and E_0' gaps, we have fitted the experimental points with the sum of Eq. (22) and of equations

$$[\epsilon_i(\omega)]_0'=\tfrac{3}{2}A_0 f_{ib}'(x_0,\gamma_0)H(\omega-5.5)\ , \tag{30}$$

$$[\epsilon_i(\omega)]_2=A_2\frac{\gamma_2 x_2}{(1-x_2^2)^2+\gamma_2^2 x_2^2}H(\omega-7.1)\ , \tag{31}$$

i.e., we consider that the contribution of the E_0' gap starts at 5.5 eV and that of the E_2 gap at 7.1 eV. We have used $\tilde{\omega}_{\rm ID}=5.5$ eV, $\omega_0=7.1$ eV, and $A_{\rm ID}$, $\tilde{\gamma}_{\rm ID}$, A_0, γ_0, ω_2, A_2, and γ_2 as free parameters. Their values are presented in the third column of Table I. The results of the fitting are shown in Figs. 5 and 6 by solid curves.

In order to check the self-consistency of the results, we have repeated the fitting simultaneously for both, $\epsilon_r(\omega)$ and $\epsilon_i(\omega)$. The parameters obtained are presented in the fourth column of Table I. The results are shown in Fig. 7 together with the data. The results of the fitting turn out to be consistent within 5%.

IV. DISCUSSION

We have used an extended parabolic-band model to describe the experimentally available dispersion of the real and imaginary part of the dielectric function of diamond. Contributions from all primary gaps ($E_{\rm ID}$,E_0',E_2) and from the electronic plasma have been considered. The results are shown in Figs. 4–7 and are in satisfactory agreement with the data. The apparent deviation in $\epsilon_r(\omega)$ of Fig. 4 around the minimum at 12.5 eV may be due to experimental reasons. [It should be noted in this regard, that in the earlier reflectivity data of Philipp and Taft[30] the minimum value of $\epsilon_r(\omega)$ appears less deep than the present one.] We have found that the plasma contribution improves significantly the dispersion at higher energies. A similar contribution has not been taken into account in other materials of the diamond- or zinc-blende-type materials.[12–14] [In the case of GaP, for instance, Adachi[12] finds $A_0=3.03$, $A_1=6.35$, $\gamma_1=0.016$, $A_2=2.08$, $\gamma_2=0.132$, and $A_c=-0.9$. We have repeated this fitting including the plasma contribution ($\omega_p=16.5$ eV) and found $A_0=2.03$, $A_1=6.61$ $\gamma_1=0.01$, $A_2=2.14$, $\gamma_2=0.12$, and $\gamma_p=0.66$.] As shown in Fig. 5, the fitting is not satisfactory at higher energies, where $\epsilon_i(\omega)$ is expected to decrease gradually as ω^{-3} (because of the plas-

TABLE I. Values of the various parameters obtained from the fitting to the data of the theoretical expressions for $\epsilon_r(\omega)$ and $\epsilon_i(\omega)$, independently (second and third column), and simultaneously (fourth column). We have used $\tilde{\omega}_{\rm ID}=5.5$ eV, $\omega_0=7.1$ eV, $\omega_p=31$ eV.

Parameter	$\epsilon_r(\omega)$	$\epsilon_i(\omega)$	$\epsilon_r(\omega),\epsilon_i(\omega)$
$A_{\rm ID}$		0.1	0.1
$\tilde{\gamma}_{\rm ID}$		2×10^{-3}	2×10^{-3}
A_0	10.0	7.0	7.7
γ_0	0.001	0.001	0.001
ω_2 (eV)	11.7	11.7	11.7
A_2	2.7	2.8	2.8
γ_2	0.170	0.175	0.175
γ_p	0.675		0.925

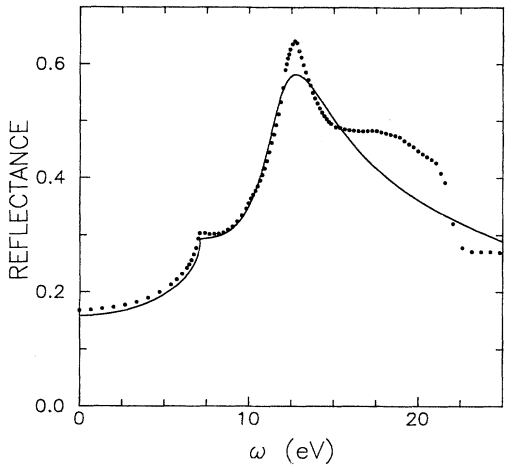

FIG. 8. Reflectance of diamond for incident photon energies in the range 0 to 25 eV. Solid curve: results of present calculation based on calculated values of $\epsilon_r(\omega)$ and $\epsilon_i(\omega)$ from Fig. 7. Dots: experimental points (after Ref. 2).

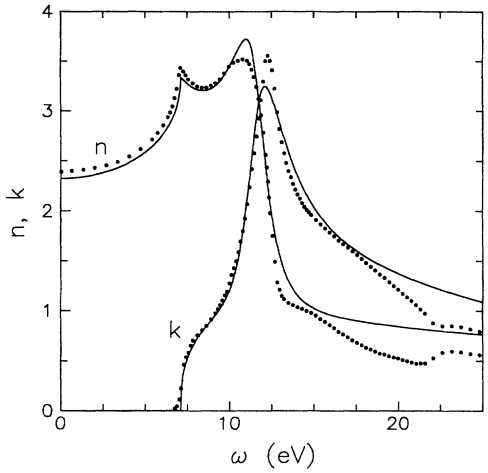

FIG. 9. As in Fig. 8 for the index of refraction (n) and the extinction coefficient (k) of diamond. Dots: values calculated from experimental points for $\epsilon_r(\omega)$ and $\epsilon_i(\omega)$ of Ref. 2.

ma contribution), tending to zero at about $\omega=\omega_p$. Instead, a long tail appears to persist in the fitted curve. This is attributed to the contribution of the E_0' gap, which imposes on $\epsilon_i(\omega)$ a slower ($\omega^{-3/2}$) dependence on the frequency. Finally, it is seen from Fig. 6 that the model explains satisfactorily the $\epsilon_i(\omega)$ dispersion immediately above the fundamental absorption edge.

In Fig. 8 we present the experimental and fitted values for the reflectance of diamond and, likewise, for the index of refraction and for the extinction coefficient in Fig. 9. With the exception of the high-energy region where the same deviations commented above appear to persist, the experimental points and the results of the present model are in satisfactory agreement.

ACKNOWLEDGMENTS

Partial support of this work was provided by the General Secretariat for Research and Technology, Greece. Discussions with S. Logothetidis and S. Papadopoulos are acknowledged with appreciation.

[1]R. Messier and W. Yarbrough, Phys. Today **42**(1), S-65 (1989), and references therein.
[2]H. R. Philipp and E. A. Taft, Phys. Rev. **136**, A1445 (1964).
[3]R. A. Roberts and W. C. Walker, Phys. Rev. **161**, 730 (1967).
[4]D. M. Roessler, Brit. J. Appl. Phys. **16**, 1119 (1965).
[5]M. Cardona, J. Appl. Phys. **32**, 2151 (1961).
[6]H. Ehrenreich, H. R. Philipp, and J. C. Phillips, Phys. Rev. Lett. **8**, 59 (1962).
[7]M. Cardona, J. Appl. Phys. **36**, 2181 (1965).
[8]L. I. Korovin, Fiz. Tverd. Tela (Leningrad) **1**, 1311 (1959) [Sov. Phys.—Solid State **1**, 1202 (1959)].
[9]M. Cardona, in *Solid State Physics, Nuclear Physics and Particle Physics,* edited by I. Saavedra (Benjamin, New York, 1968).
[10]M. Cardona, *Modulation Spectroscopy* (Academic, New York, 1969).
[11]C. W. Higginbotham, M. Cardona, and F. H. Pollak, Phys. Rev. **184**, 821 (1969).
[12]S. Adachi, Phys. Rev. B **35**, 7454 (1987).
[13]S. Adachi, Phys. Rev. B **38**, 12 966 (1988).
[14]S. Adachi, J. Appl. Phys. **66**, 813 (1989).
[15]D. T. F. Marple and H. Ehrenreich, Phys. Rev. Lett. **8**, 87 (1962).
[16]F. Stern, Phys. Rev. **133**, A1653 (1964).
[17]S. H. Wemple and M. DiDomenico, Jr., Phys. Rev. B **3**, 1338 (1971).
[18]A. N. Pikhtin and A. D. Yas'kov, Fiz. Tekh. Poluprovodn. **12**, 1047 (1978) [Sov. Phys.—Semicond. **12**, 622 (1978)].
[19]D. L. Greenaway and G. Harbeke, *Optical Properties and Band Structure of Semiconductors* (Pergamon, London, 1968).
[20]M. Cardona, in *Atomic Structure and Properties of Solids,* edited by E. Burnstein (Academic, New York, 1972), p. 514.
[21]J. N. Hodgson, *Optical Absorption and Dispersion in Solids* (Chapman and Hall, London, 1970).
[22]J. Bardeen, L. H. Hall, and F. J. Blatt, in *Photoconductivity Conference,* edited by E. Breckeneridge (Wiley, New York, 1954).
[23]C. D. Clark, P. J. Dean, and P. V. Harris, Proc. R. Soc. London, Ser. A **277**, 312 (1964).
[24]R. Robertson, J. J. Fox, and A. E. Martin, Proc. R. Soc. London, Ser. A **157**, 579 (1936).
[25]C. D. Clark, R. W. Ditchburn, and H. B. Dyer, Proc. R. Soc. London, Ser. A **234**, 363 (1956).
[26]W. Kaiser and W. L. Bond, Phys. Rev. **115**, 857 (1959).
[27]J. F. H. Custers, Physica **18**, 489 (1952).
[28]E. Anastassakis, Phys. Rev. **186**, 760 (1969).
[29]J. R. Nelson and W. C. Crocker, Bull. Am. Phys. Soc. **5**, 431 (1960).
[30]H. R. Philipp and E. A. Taft, Phys. Rev. **127**, 159 (1962).
[31]W. C. Walker and J. Osantowski, Phys. Rev. **134**, A153

(1964).
[32]H. Armon and J. P. F. Sellschop, Phys. Rev. B **26**, 3289 (1982).
[33]D. M. Roessler, Ph.D thesis, King's College, London, 1966 (unpublished).
[34]W. Saslow, T. K. Bergstresser, and Marvin L. Cohen, Phys. Rev. Lett. **16**, 354 (1966).
[35]F. Herman, R. L. Kortum, C. D. Kuglin, and R. A. Short, J. Phys. Soc. Jpn. Suppl. **21**, 7 (1966).
[36]F. J. Himpsel, J. F. van der Veen, and D. E. Eastman, Phys. Rev. B **22**, 1967 (1980).
[37]N. R. Whetten, Appl. Phys. Lett. **8**, 135 (1966).
[38]F. Peter, Z. Phys. **15**, 358 (1923); *Physics of Group IV Elements and III-V Compounds,* Vol. 17a of *Landolt-Börnstein, New series, Group III,* edited by O. Madelung (Springer-Verlag, Berlin, 1982), p. 36.
[39]C. J. Rauch, in *Proceedings of the International Conference on the Physics of Semiconductors, Exeter, 1962,* edited by A. C. Strickland (Institute of Physics and the Physical Society, London, 1962), p. 276.